Annals of Biomedical Engineering, Vol. 37, No. 8, August 2009 (© 2009) pp. 1572–1583
DOI: 10.1007/s10439-009-9724-z

An Experimental and Theoretical Study on the Anisotropy of Elastin Network

YU ZOU[1] and YANHANG ZHANG[1,2]

[1]Department of Mechanical Engineering, Boston University, 110 Cummington Street, Boston, MA 02215, USA; and [2]Department of Biomedical Engineering, Boston University, 44 Cummington Street, Boston, MA 02215, USA

(*Received 19 November 2008; accepted 21 May 2009; published online 30 May 2009*)

Abstract—The mechanical properties of elastin network from bovine thoracic aorta under biaxial tensile loading were studied both experimentally and theoretically. Histology and scanning electron microscopy were performed to verify the removal of cells, collagen, and other extracellular matrix components. Equi- and nonequi-biaxial tests were performed to study the effect of different loading conditions on the stress–strain responses of the elastin network. The mechanical properties of different elastin sections along the thoracic aorta were examined and studied to understand the anisotropy of elastin along the whole artery. Biaxial tensile test data comparing elastin vs. intact aorta showed that elastin is mainly responsible for the linear elastic response of the arterial wall at lower strains. Experimental results revealed that elastin network possesses significant anisotropic mechanical properties with the circumferential direction being stiffer than the longitudinal direction. The mechanical properties of elastin vary significantly along the thoracic aorta, with the thin section appearing to have the highest tangent modulus. Biological assay results indicate that elastin content is about the same along the thoracic aorta. The mechanical behavior of elastin network was well captured by the eight-chain statistical mechanics based microstructural model. Material parameters obtained from the equi-biaxial test were able to predict the stress–strain responses of elastin network under arbitrary nonequi-biaxial loading conditions. Also, by varying material parameters in the model, the changes in microstructure such as elastin fiber orientation and cross-linking density on the macroscopic mechanical properties of elastin network were discussed.

Keywords—Elastin network, Extracellular matrix, Orthotropic hyperelasticity, Cross-linking density, Fiber orientation, Fiber density, Microstructural model.

INTRODUCTION

Blood vessels are complex organs with hierarchical ultrastructures. Extracellular matrix (ECM) and smooth muscle cells (SMCs) bear the vast majority of wall stress and determine the mechanical and chemical properties of the blood vessels. Elastic fibers are one of the major ECM assemblies that endow blood vessels critical mechanical properties such as flexibility and extensibility,[17] and are essential to accommodate deformations encountered during physiological functions. These resilient network structures are made primarily of a protein–elastin. Many Pathological conditions such as cardiovascular diseases, aortic aneurysms, aging of connective tissues, etc., involve significant remodeling and degradation of elastin. Biological remodeling mechanisms of blood vessels due to cardiovascular diseases have been studied for the past three decades.[29,37,42] Rapid synthesis of collagen and elastin in blood vessels has been found by many biological studies in both systemic and pulmonary hypertensions. Thickening of the arterial wall has been correlated to the hypertrophy of SMCs, extracellular connective tissue, and collagen and elastic fibers. Loss of elasticity due to degradative changes in elastin is found to be a major contributing factor in the development of aortic aneurysms, in ageing of connective tissues, and in lung emphysema.[27,34,38]

The microstructural remodeling is greatly associated with its altered mechanical properties. Elastin network in blood vessels plays a significant role in modifying the mechanical behavior of these dynamic soft tissues. However, the mechanical properties of elastin are not fully understood, and studies connecting microstructural changes with elastin mechanics are lacking. In a few previous studies the mechanical loading has been limited to simple uniaxial stretching,[22,23] which ignores the multiaxial loading state under physiological conditions, and cannot fully characterize the intrinsic orthotropic nature of soft biological tissue.

To model the complex mechanical behavior of soft biological tissues, most investigators have relied on phenomenological approaches.[8,10,13–15,36,43] These strain energy functions utilize a continuum mechanics approach and are either invariants based or principal-

Address correspondence to Yanhang Zhang, Department of Mechanical Engineering, Boston University, 110 Cummington Street, Boston, MA 02215, USA. Electronic mail: yanhang@bu.edu

stretch based.[15] In these phenomenological constitutive models, mathematical functions are chosen to describe the mechanical behavior of the biological tissue, but the parameters in the model do not possess any physical meanings.[31] Thus the relations connecting micro-level structural properties with tissue-level mechanics are lacking. Strain energy functions of polynomial, exponential, and logarithmic forms were proposed in the literature to capture the hyperelastic response of arteries. Holzapfel and Gasser[13] provided an excellent review and assessment of a range of two- and three-dimensional models.

Constitutive models based on non-Gaussian affine statistical characterization of a network of randomly oriented molecular chains are also proposed in the literature to provide microstructural information. Entropy-based constitutive laws were used to model the mechanical response of a single molecular chain. The essential idea is that the mechanical response of the material is due to an underlying molecular network structure, which relates the mechanical response at macro-level to the deformation (entropy change) of individual molecular chains at the micro-level. Specific network models composed of three-chain,[16] four-chain,[9] and eight-chain[2,3] unit elements are proposed to model a network of molecular chains to obtain a continuum behavior. Zhang *et al.*[44] have recently applied the statistical mechanics based microstructural model to study the orthotropic hyperelastic behavior of pulmonary artery mechanics with pulmonary arterial hypertension. This study connects micro-level changes with whole-artery mechanics and sheds light on the relationship between the change in artery mechanics and the potential change in microstructure for pulmonary arterial hypertension.

The objective of this study is to fully understand the macroscopic elastic behaviors of elastin network using combined experimental and modeling approaches and relate mechanical behaviors to its microstructure. The anisotropic mechanical property of isolated bovine aortic elastin is studied experimentally using planar biaxial tensile testing, then theoretically using a statistical mechanics-based orthotropic hyperelastic constitutive model that was previously implemented. Material parameters in the constitutive model are expected to be related with the microstructure of elastin network.

MATERIALS AND METHODS

Sample Preparation

Fresh young bovine (average weight of 80 lbs) thoracic aortas were harvested from a local abattoir. Experiments were done within 24 h of harvesting to minimize the effect of degradation of the microstructural components in the artery. The aortas were cleaned of adherent tissues and fat, dissected, rinsed in DI water, and cut into squares of about 2 cm × 2 cm sections along the aorta. The thickness of the aorta decreases from the proximal to the distal end. Square tissue samples were obtained and grouped into thick, medium and thin sections with the thick sections located nearer to the proximal end and the thin section nearer to the distal end of the thoracic aorta. Tissue samples were kept in 1× phosphate buffered saline (PBS) for further experiments.

Elastin networks were isolated following the procedure developed previously by Lu *et al.*[26] In this procedure, collagen fibers and other extracellular matrix components were removed by cyanogen bromide (CNBr) treatment. Briefly, fresh aorta samples were immerged in 50 mg/mL CNBr in 70% formic acid solution. Approximately 8 mL solution is needed per square centimeter of tissue sample. The samples were treated for 19 h at room temperature with gentle stirring. Then, they were gently stirred for 1 h at 60 °C and followed by 5 min of boiling in order to inactivate CNBr. Samples were rinsed in DI water and kept in PBS before mechanical testing.

Isolated elastin networks from six bovine aortas were tested in this study. For each isolated elastin sample, the corresponding aorta from adjacent location was also tested for the purpose of comparison. The thickness of the tissue was measured at nine different locations across the square sample and averaged. The thicknesses of the thick, medium and thin sections are 2.41 ± 0.27, 1.52 ± 0.08, and 1.12 ± 0.15 mm, respectively, for the aorta samples; and 1.70 ± 0.21, 1.07 ± 0.11, and 0.49 ± 0.03 mm, respectively, for the elastin samples.

Scanning Electron Microscopy (SEM)

Surface morphology was examined using a JOEL JSM-6100 SEM operated at 5 kV. Prior to SEM, the samples were fixed in Karnovsky's fixative kit (2% paraformaldehyde, 2.5% glutaraldehyde and 0.1 M sodium phosphate buffer, Fisher Scientific) for 1 h and then dehydrated in a series of graded ethanol. The samples were then dried using Denton vacuum DCP-1 CO_2 critical point dryer. A very thin layer of platinum was coated on the cross-section of the samples using Sputter Coater (Cressington 108).

Histology

Histological images of the cross-section of the tissue samples were taken to validate the removal of SMCs and other ECM components in the isolated elastin network.

Tissue samples were fixed in 10% formalin buffer and then embedded in paraffin. Sections of about 6 μm in thickness were obtained and stained with Hematoxylin and Eosin (H&E), and Masson's trichrome. The H&E stains cell nuclei dark purple, and elastin, collagen and other ECM pink. Masson's trichrome stains elastin fiber red, cell nuclei dark red, and collagen blue.

Elastin Assay

After biaxial tensile testing, elastin content in intact aorta and isolated elastin network was measured using Fastin^{TM} elastin assay (Biocolor Ltd., Northern Ireland) following manufacture's protocols. The optical density was measured at 513 nm using a SpectraMax M5 microplate reader. Elastin content was normalized to tissue wet weight and expressed as μg elastin/mg tissue.

Biaxial Tensile Testing

Since biological tissues are usually considered incompressible, planar biaxial tensile testing can be used to fully characterize the mechanical properties.[15,33] Tissue samples of about 2 cm × 2 cm were sutured at the side and loaded biaxially.[32] Briefly, the square specimens were hooked on four sides using fishing hooks that are attached to nylon sutures, as seen in Fig. 1. The nylon sutures are connected to specially designed carriages that allow for self-equilibrated loads for each suture line. Four markers made by oil-based permanent marker forming an approximately 5 mm × 5 mm square were placed in the center of the sample, and a CCD camera (resolution of 0.02 mm/pixel) were used to trace the markers and determine the strains in both loading directions throughout the deformation. Before the testing, load cells were calibrated using standard known loads. The distances between hooks in both longitudinal and circumferential directions were measured and used in the finite element model.

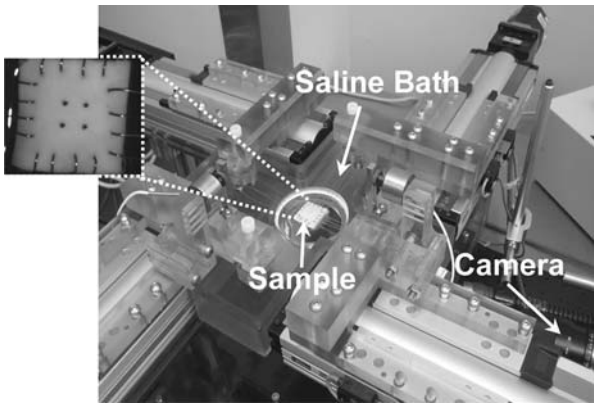

FIGURE 1. Picture of the biaxial tensile tester. The sample is mounted using sutures hooked to each side. The system has a custom-designed bath to keep the sample in a liquid environment during testing.

Tissue samples were preconditioned for 8 cycles with 15 s of half cycle time equi-biaxially to obtain repeatable material response. Each sample was then subjected to both equi- and nonequi-biaxial tensile test using load control. Every test trial consisted of 10 cycles to allow the biomaterial exhibiting repeatable loading and unloading curve. The force–stretch response in both directions was recorded. Cauchy stresses vs. logarithm strain were used to describe the mechanical behavior of aorta and elastin network. The logarithm strain is obtained by taking the natural logarithm of stretch. The Cauchy stresses in the longitudinal (x_1) and circumferential (x_2) directions of the tissue sample are obtained by:

$$\sigma_1 = \frac{F_1\lambda_1}{hL_{02}}, \qquad \sigma_2 = \frac{F_2\lambda_2}{hL_{01}} \tag{1}$$

where σ_i ($i = 1, 2$) is the Cauchy stress, F_i and λ_i ($i = 1, 2$) represents the load and stretch in the x_i direction; h and L_{0i} ($i = 1, 2$) are the original thickness and length, respectively, of the sample before it was stretched. After preconditioning, a small preload is applied to ensure flatness and tautness of the soft tissue. This preloaded state is also used as the reference state for later stress and strain measurement.

Constitutive Modeling

The stress–strain response of elastin network was modeled using a statistical mechanics-based orthotropic hyperelastic microstructural model that was previous implemented using finite element method.[44] The model provides an analogy between the entangled long molecular chains and the structural protein framework seen in the elastin network. The eight-chain element is selected as the basic unit while every single chain is modeled as a freely joined chain; these can have different dimensions in the three orthogonal material directions and in this manner, the response of the unit element is made orthotropic. The unit element can then be homogenized to form the strain energy function of the material. The final form of the strain energy function is[3]:

$$w = w_0 + \frac{nk\Theta}{4}\left[N\sum_{i=1}^{4}\left(\frac{\rho^{(i)}}{N}\beta_\rho^{(i)} + \ln\frac{\beta_\rho^{(i)}}{\sinh\beta_\rho^{(i)}}\right) - \frac{\beta_p}{\sqrt{N}}\ln\left(\lambda_1^{a^2}\lambda_2^{b^2}\lambda_3^{c^2}\right)\right] + B[\cosh(J-1)-1] \tag{2}$$

where w is the overall energy, w_0 is a constant, B is a parameter that controls the bulk compressibility and J is the determinant of deformation gradient tensor. Parameters a, b, and c are normalized dimensions along the principal material directions, and λ_1, λ_2, and λ_3 are stretches along these directions. $N = \frac{a^2+b^2+c^2}{4}$ is the number of links within each individual chain. $\rho^{(i)}$ are the normalized deformed lengths of the constituent chains in the unit element. $\beta_\rho^{(i)} = \ell^{-1}\left(\rho^{(i)}/N\right)$ is the inverse Langevin function. $p = \frac{1}{2}\sqrt{a^2+b^2+c^2}$ is the initial normalized length of each chain. Parameter n is the chain density per unit volume; k is Boltzmann's constant; and Θ is absolute temperature. Interested readers are referred to Bischoff *et al.*[3] and Zhang *et al.*[44] for more detailed explanations about the model.

It is useful to relate the input material parameters in the model with the microstructure and the mechanical behavior of the elastin network. There are four independent material parameters in the model: *a, b, c* and *n*. The *a* and *b* material axes are aligned along the longitudinal and circumferential directions of the arterial wall, respectively. As shown in the representative stress–strain curves in Fig. 2a, the relative values of *a*, *b* and *c* provide information on the fiber orientation and the degree of orthotropy that exists in the network. $N = \frac{a^2+b^2+c^2}{4}$ is related to the chain length between the two cross-links at micro-level, and the extensibility of the material at macro-level. A less extensible material will be expected to be more cross-linked and thus have a smaller N. The chain density per unit volume, n, is related to the elastin content, and the initial tangent modulus of the elastin network. Interested readers are referred to Zhang *et al.*[44] for more discussions on the choice and sensitivity of individual material parameters.

Due to the symmetric loading conditions in biaxial tensile testing, a quarter of the sample was modeled in Abaqus 6.7 to simulate the biaxial stretching of the square sample, as shown in Fig. 2b. Shell edge load was applied on two sides of the model to simulate the biaxial loading. *x*- and *y*-symmetry boundary conditions were applied on the other two sides of the model. General-purpose shell elements (S4R) with inherent plane stress assumption were used in the finite element model. A characteristic mesh size of about 0.4 mm was chosen after a mesh-validation study to optimize between convergence rates and mesh resolution.

Material parameters in the finite element model were adjusted to fit the experimental data. The correlation coefficient r^2 of the modeling results based on the orthotropic hyperelastic microstructural model compared to the experimental data was calculated by the ratio of the mean square error (*MSE*) to the

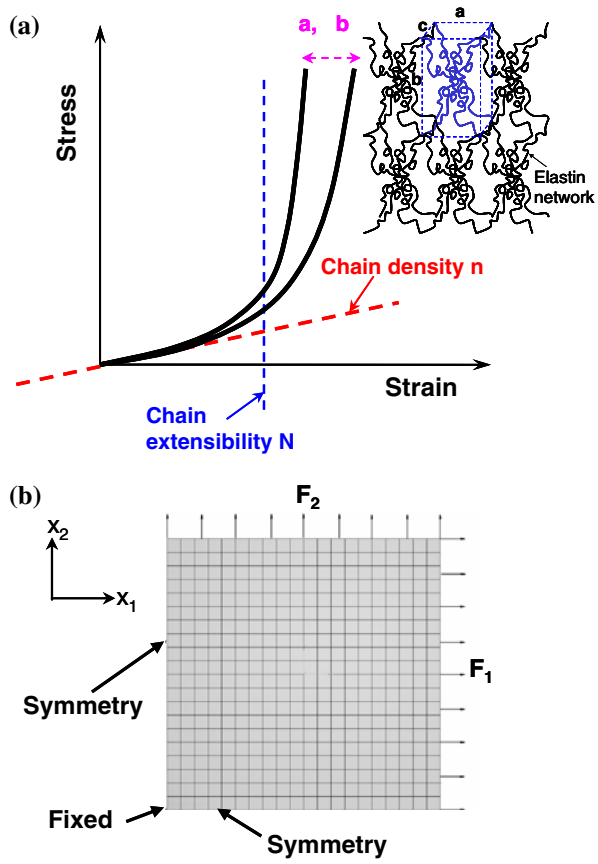

FIGURE 2. (a) Representative hyperelastic orthotropic stress–strain responses with model parameters related to the microstructure and mechanical behavior of the elastin network and (b) the finite element model with boundary and loading conditions.

variance of the experimental data,[11] i.e., $r^2 = 1 - MSE/Var\sigma_i$, where σ_i is the Cauchy stress experimental data obtained from Eq. (1). To determine *MSE*, the modeling results of Cauchy stress vs. logarithm strain were first interpolated and used to obtain the residuals between the experimental data and interpolated modeling results.

RESULTS

Upon removal of cells, collagen fibers and other ECM components, the isolated elastin appears to be a more porous structure, as can be seen from Fig. 3. SEM image of isolated elastin in Fig. 4 reveals regularized concentric layer of elastin sheets, which are less obvious with the presence of collagen fibers and smooth muscle cells in the intact aorta. Histology images in Fig. 5 demonstrate the apparent difference in the microstructure of bovine aorta and its corresponding elastin. Samples stained with H&E show that the elastin samples are empty of cells compared to intact aorta

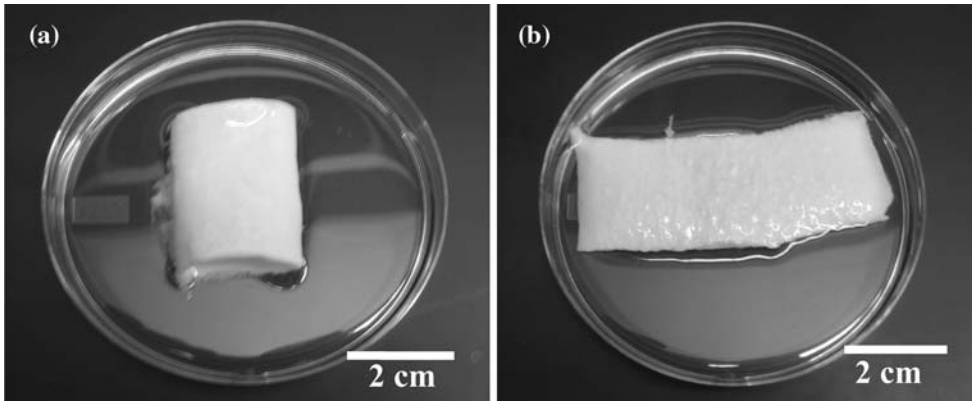

FIGURE 3. Images of segments of (a) bovine thoracic aorta and (b) isolated elastin network.

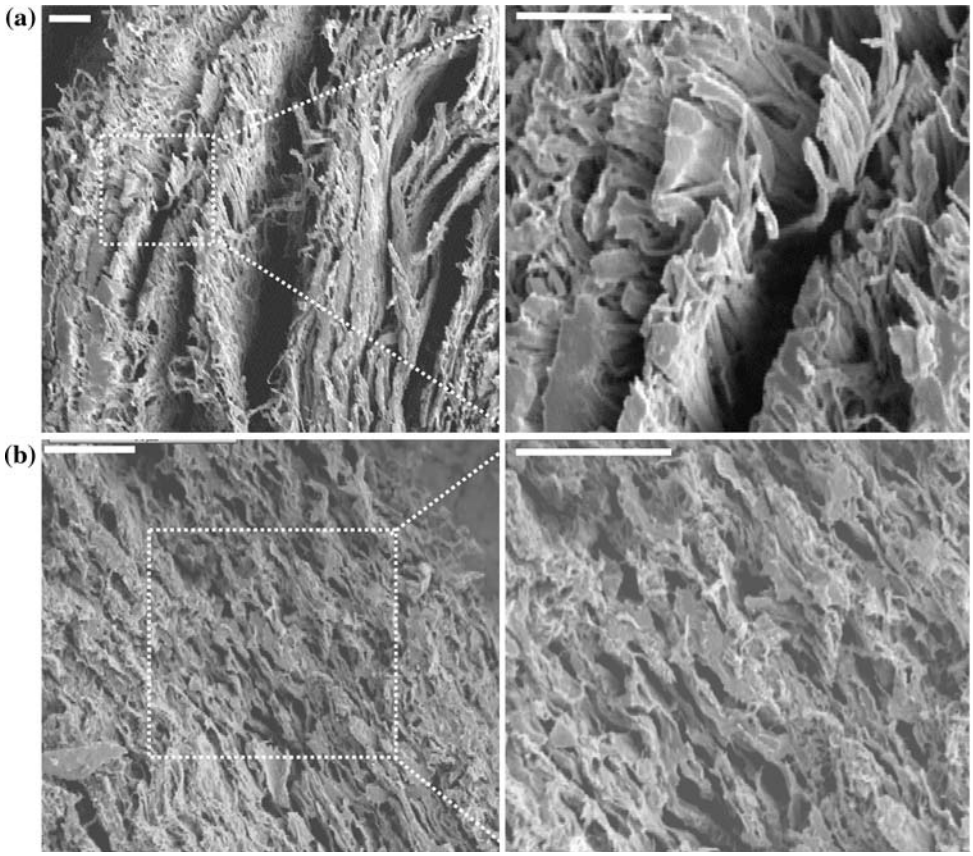

FIGURE 4. Scanning electron microscopy (SEM) images of (a) isolated elastin network and (b) intact bovine thoracic aorta. All scale bars represent 20 μm.

samples; also, elastin samples have lower density of 3-D ECM network. The Masson's trichrome stain of the aorta samples shows cells embedded in a cross-linked network of elastin and collagen fibers; while the same stain of elastin samples shows that only elastic fibers present in the isolated elastin network. The Masson's trichrome stain also showed that the fibers in elastin sample are less dense than in the intact aorta.

Figure 6 shows that the elastin content in isolated elastin is about twice of that in the companion aorta for samples from thick, medium, and thin sections. The isolation of elastin increases the elastin concentration by removing SMCs, collagen, and other ECM components. The reason that the aortas from the medium section have slightly higher elastin concentration than the thick and thin section is unclear. However the

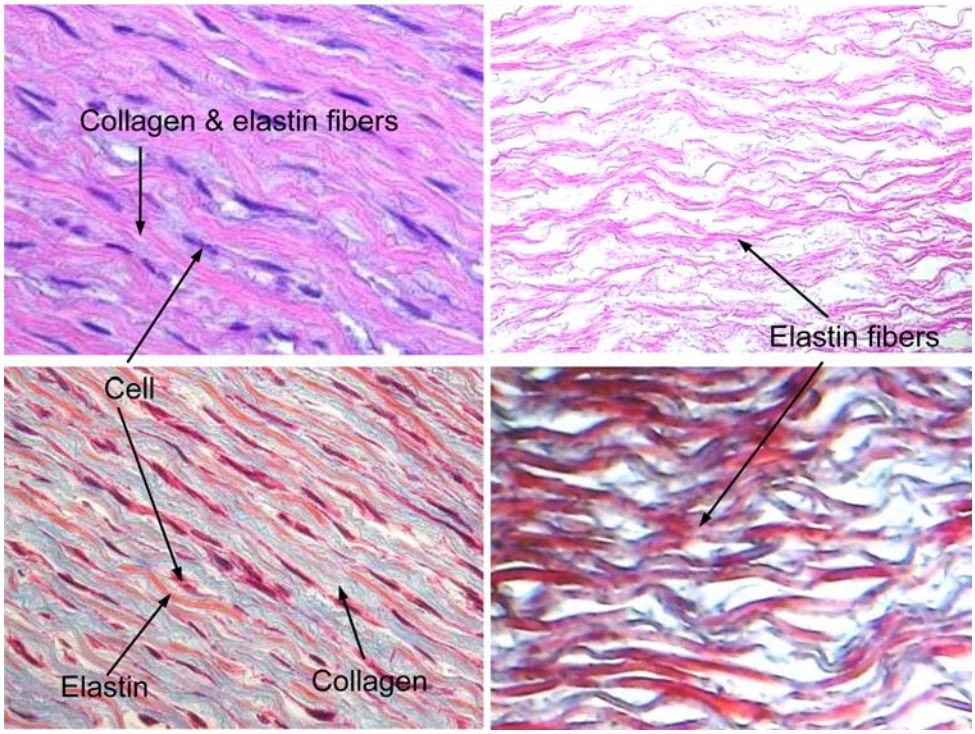

FIGURE 5. Histology pictures showing the H&E stain (up) and Masson's trichrome stain (down) of intact thoracic aorta (left) and isolated elastin (right).

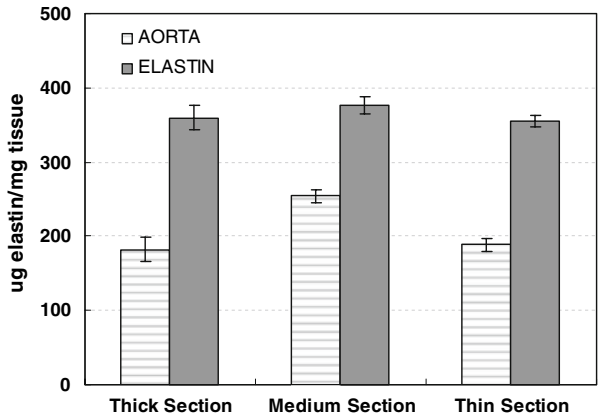

FIGURE 6. Elastin concentration of aorta samples and isolated elastin network from the thick, medium and thin sections. Data are mean ± SE, $n = 5$.

elastin concentration of the isolated elastin is about the same for all the sections.

Figure 7a shows the representative stress–strain response of aorta and its elastin from the medium section of the bovine aorta under equi-biaxial test with loads of 150 and 50 g, respectively. The biaxial tensile test reveals the anisotropic mechanical properties of both the artery and its elastin with circumferential direction being stiffer than the longitudinal direction. Anisotropy in blood vessel is not a surprise. However to the best of our knowledge, orthotropic response in the aortic elastin network has not been reported before. The experimental results show consistently that elastin network possesses strong anisotropy that is comparable to the intact arteries. The biaxial tangent modulus was extracted under equi-biaxial plane-stress assumptions by differentiating the stress–strain curve.[44] For nearly incompressible material, the biaxial tangent modulus can be estimated from $E_t \approx 1/2 d\sigma/d\varepsilon$, and is plotted in Fig. 7b.

Figure 8 shows the effect of different loading conditions on the stress–strain responses of elastin network. Equi- and nonequi-biaxial tests were performed. Since elastin is stiffer in the circumferential direction, uneven loading with higher load in the circumferential direction reduces the degree of anisotropy in the stress–strain responses. On the other hand, uneven loading with higher load in the softer longitudinal direction increases the anisotropy in the stress–strain responses. Although not shown here, the stress–strain responses of aorta show the same trend.

To understand the anisotropic mechanical behavior of elastin along the thoracic aorta, elastin samples from the thick, medium, and thin sections of the thoracic aorta were tested. Figure 9 shows the stress–strain curves of elastin networks from different sections under equi-biaxial tensile tests. The experimental results show that the mechanical properties of elastin

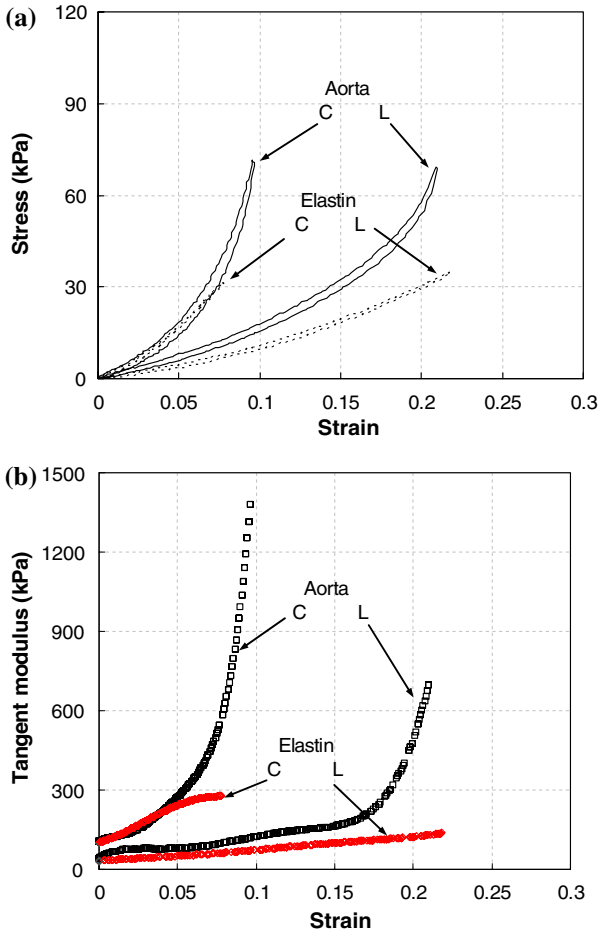

FIGURE 7. (a) Cauchy stress vs. logarithmic strain for the aorta sample and its elastin network from the medium section of the bovine thoracic aorta under equi-biaxial loading. The load is 150 and 50 g for aorta and elastin, respectively. (b) Corresponding tangent modulus vs. logarithmic strain for aorta and elastin network. L represents longitudinal direction, and C represents circumferential direction throughout the paper.

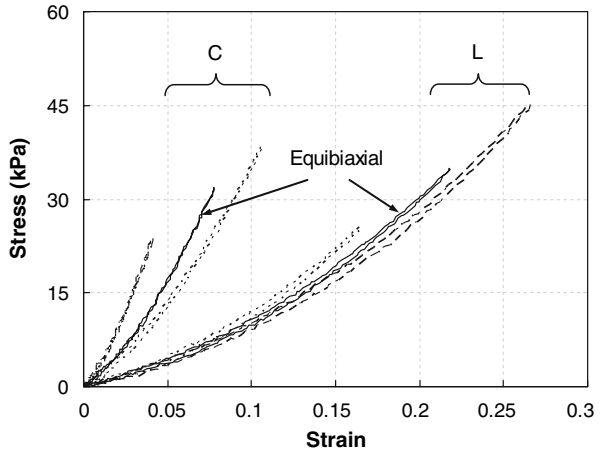

FIGURE 8. Cauchy stress vs. logarithmic strain for elastin network from the medium section of the bovine thoracic aorta under equi- and nonequi-biaxial loading. The solid lines represent 50 g load in both the L and C directions; dotted lines represent 40 g load in the L direction and 60 g load in the C direction; and dashed lines represent 60 g load in the L direction and 40 g load in the C direction.

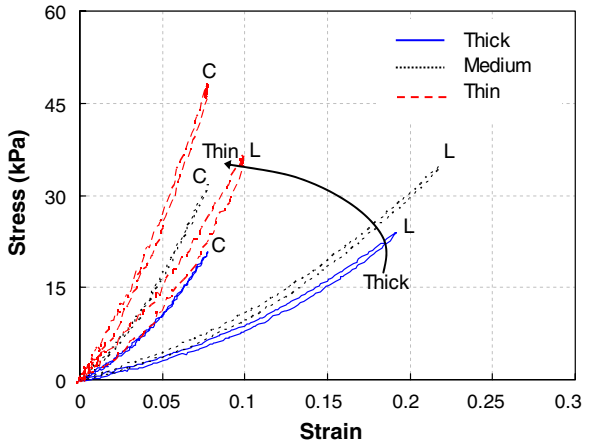

FIGURE 9. Cauchy stress vs. logarithmic strain for elastin network from the thick, medium and thin sections of the bovine thoracic aorta under equi-biaxial loading. The load is 50 g for thick and medium sections, and 25 g for thin section.

vary along the thoracic aorta. In both the longitudinal and circumferential directions, the thinner sections always have a higher tangent modulus than the thicker sections. Again, results from aorta show a similar trend with thinner sections being stiffer than the thicker sections.

Figure 10 shows the simulation results of equi- and nonequi-biaxial test of elastin network. Experimental results were also plotted for the purpose of comparison. Material parameters were obtained by fitting the simulation results to the equi-biaxial test data ($r^2 = 0.9911 \pm 0.0038$). These material parameters were then used to predict the mechanical responses under nonequi-biaxial loading conditions and compared with experimental results ($r^2 = 0.9504 \pm 0.0460$). Figure 10 shows that the material parameters obtained from the equi-biaxial test were able to predict the stress–strain responses of elastin network under arbitrary nonequi-biaxial loading conditions. These results confirm that the microstructural model is suitable for the study of the anisotropic hyperelastic mechanical behavior of elastin network.

DISCUSSIONS

Fully elucidation of the structure–function relationships of elastin network are critical in many areas of research of understanding physiological and pathological conditions in native blood vessels, creating

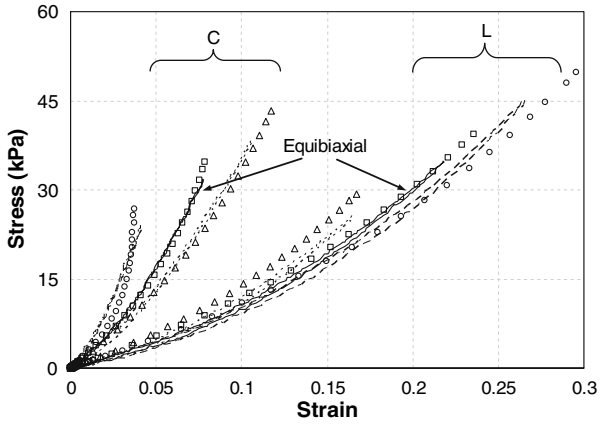

FIGURE 10. Simulation results of Cauchy stress vs. logarithmic strain for elastin network under equi- and nonequi-biaxial loading, represented by symbols. Experimental results from Fig. 8 were shown for the purpose of comparison and represented by lines. Material parameters were obtained by fitting simulation results to equi-biaxial tests. $n = 5.8 \times 10^{15}$ (1/mm^3), $a = 1.31$, $b = 1.8011$, $c = 1.2$, $N = 1.6$, $k = 1.38 \times 10^{-23}$ J/K, and $T = 298$ K.

functional scaffolds in tissue engineering, and illuminating the interactions between cell and ECM. Results from this study established a foundation to investigate the role of microstructural components on the functionality of blood vessels. Currently, there are few constitutive models that describe arterial mechanical behavior based on its microstructure. Microstructural-based models have the potential to increase the ability of mathematical and computational models to describe and predict physiological and pathophysiological responses of blood vessels. Study from Rezakhaniha and Stergiopulos[31] concluded that anisotropic elastin behavior is required for the more success of structural models. However, the anisotropic properties of individual microstructural components are not currently available. This study would be a substantial step toward developing microstructural models.

Various methods for the isolation of elastin have been developed depending on its insolubility, chemical inertness and resistance to hydrolysis. Interested readers can refer to Daamen *et al.*[5,7] and Mecham[28] for reviews. The elastin purification method adopted in this study was first introduced by Rasmussen *et al.*[30] It has been adapted and demonstrated to be simple and effective by Lu *et al.*[26] and others.[19,35] It is expected that the experimental and theoretical methods developed in this study are applicable to the elastin network obtained from other purification methods as well.

It is well-known that blood vessels possess anisotropic material properties, i.e., the mechanical response in the circumferential and longitudinal directions are not the same. Some work has been done on the mechanical testing of the elastic and viscoelastic properties of elastin networks.[22,23,26] However, these studies have been restricted to uniaxial imposed loadings, which does not accurately reflect the state of deformation encountered in the body (both circumferential and longitudinal stretching), and are insufficient to elaborate the structurally and mechanical anisotropy seen in blood vessels. A few research groups have used the biaxial tensile testing approach to test both engineered and native biological tissues, such as native and engineered planar heart valve,[1,33] arteries,[20] collagen gels.[18] These studies have demonstrated the importance of rigorous experimental approaches on fully elaborating structural–functional responses. Gundiah *et al.*[12] performed uniaxial and equi-biaxial tensile test on isolated elastin. In their equi-biaxial tensile tests the strain was up to about 4%, within which the elastin appears to be isotropic manifested by equivalent material tangent modulus in the axial and circumferential directions. However, results of this research display anisotropy in elastin even at these low strains. This discrepancy is not clear and might be contributed to the differences in elastin isolation methods and storage. In the study by Gundiah *et al.*,[12] elastin was isolated by autoclave and hot alkali methods from porcine aorta, and then stored in 80% ethanol for about a week. The elastin samples were then washed and rehydrated in distilled water before testing. Recent research showed that the use of 70% ethanol can cause elastin tissue to swell.[24] Moreover, the mechanics of elastin has been shown to strongly correlate with its water content.[21] Studies considering these conditions are necessary in order to elucidate the cause of the aforementioned discrepancies.

The equi- and nonequi-biaxial tensile tests with finite strain revealed several interesting facts of the mechanical properties of elastin. As shown in Fig. 7a, the experimental results consistently show that elastin network possesses strong anisotropy that is comparable to the intact arteries, with the circumferential direction being stiffer than the longitudinal direction. This study also indicates that the elastin network is responsible for the linear elastic response of blood vessels under lower strains. While at higher strains, the aorta becomes much stiffer in both directions due to the strain stiffening and the involvement of collagen fibers, and the stress–strain responses of intact aorta are more nonlinear compared with the elastin.

The aorta and elastin network has similar tangent modulus in the circumferential direction when strain is below 5%. The initial tangent modulus is about 100 kPa and it increases almost linearly to 200 kPa at 5% of strain. As the strain further increases, the tangent modulus of aorta increases dramatically and results in a much higher modulus. The tangent modulus in the circumferential direction at the physiological

strains is consistent with previous *in vivo* and *in vitro* studies on aortic mechanics[40,41,44] in which the tangent modulus at low tensile strains were shown to vary from 100 to 350 kPa. The tangent modulus in the longitudinal direction is significantly lower than that in the circumferential direction. The elastin network has an initial tangent modulus of about 30 kPa. The tangent modulus of aorta is about twice as that of elastin below 15% strain, and increases significantly at higher strains. These results further proved that elastin contributes to the aortic mechanics in the physiological range. The physiological strains of aortic circumferential deformation have been reported to be over 5%,[25,39] while in the longitudinal direction, the *in vivo* strain can be greater than 20%.[45] Comparison between equi-biaxial mechanics of elastin and aorta sheds light on understanding the role of the microstructural components in the mechanical behavior of the arterial wall, and making functional biological scaffolds with desired biomechanical properties. Previous studies on scaffolds with different ratios of collagen and elastin[4,6,26] have shown that scaffolds with higher collagen content had a higher tensile strength, whereas addition of elastin increased elasticity and distensibility. Results from this study provided quantitative information on the mechanical properties of elastin network compared to intact artery. Further studies on the mechanical properties of other ECM components such as collagen are underway.

The nonequi-biaxial tensile tests allow us to study the anisotropic mechanical behavior of elastin under various loading conditions, as shown in Fig. 8. Since the elastin network is stiffer in the circumferential direction than in the longitudinal direction, higher load in the circumferential direction results in reduced anisotropy in the stress–strain responses. On the other hand, higher load in the longitudinal direction results in increases anisotropy in the stress–strain responses. The simulation results from Fig. 10 demonstrate that the eight chain statistical mechanics-based microstructural model is suitable to describe and predict the elastic behavior of elastin network. The material parameters were obtained from the experimental data of equi-biaxial test, and simulations results using these parameters could predict the stress–strain responses under nonequi-biaxial loading conditions.

The elastin from the thinner sections tends to have higher tangent modulus than the thicker sections in both the longitudinal and circumferential directions, as shown in Fig. 9. This is consistent with the results from Lillie and Gosline's work.[23] Using uniaxial ring stretch test, they showed that the stiffness of purified elastin increased about 30% from proximal to distal end of pig aorta. To explain this, they suggested that the elastin might be more aligned in the circumferential direction in the thin section and thus the thin section might have higher anisotropy. However, results based on biaxial tensile test did not show that the thin section has more anisotropic stress–strain responses than the thicker sections. The reason that the mechanical properties of elastin vary along the thoracic aorta is currently not clear. Quantitative bioassay, histology, and imaging studies will help to elucidate this. The elastin content was thus measured experimentally and the effect of cross-linking density and chain orientation on the mechanical properties of elastin network was also studied. The preliminary bioassay results show that the elastin content in the thick, medium and thin sections does not have a significant difference, as shown in Fig. 6. This indicates that the change of mechanical properties of elastin along the thoracic aorta is not due to the variation of elastin content.

The material parameters in the microstructural model, such as chain density and cross-linking density, have physical meanings and can be related to the microstructure of the elastin network. In order to study the effect of cross-linking density of the elastin network on the mechanical properties, the material parameter n, which corresponding to the elastin content, was kept unchanged, and the material parameter N was varied to simulate the stress–strain relationships for the thin, medium, and thick sections. Material parameters summarized in Table 1 were obtained by matching simulations to the experimental results, as shown in Fig. 11a ($r^2 = 0.9704 \pm 0.0415$). In order to simulate the anisotropic behavior of the elastin network, b is kept to be greater than a which implies that more elastin fibers are aligned in the circumferential direction than in the longitudinal direction of the arterial wall, and thus the elastin network is more stiffer in the circumferential direction. Also material parameter c was kept smaller than both a and b, which indicates that less elastin fibers are distributed in the radial direction. From the three sets of material parameters, it can be seen that the thin section has the smallest N. Material parameter $N = \frac{a^2+b^2+c^2}{4}$ is related to the chain length between the two cross-links at micro-level, and the extensibility of the material at macro-level. A

TABLE 1. Material parameters used to simulate the stress–strain responses of elastin networks from the thick, medium, and thin sections in Fig. 11a.

	n (1/mm^3)	a	b	c	N
Thick	5.80×10^{15}	1.42	1.9219	1.3	1.85
Medium	5.80×10^{15}	1.31	1.8011	1.2	1.6
Thin	5.80×10^{15}	1.31	1.5079	1.1	1.3

Material parameter n is kept unchanged, while N is allowed to change to study the effects of cross-linking density on the mechanical properties of elastin network.

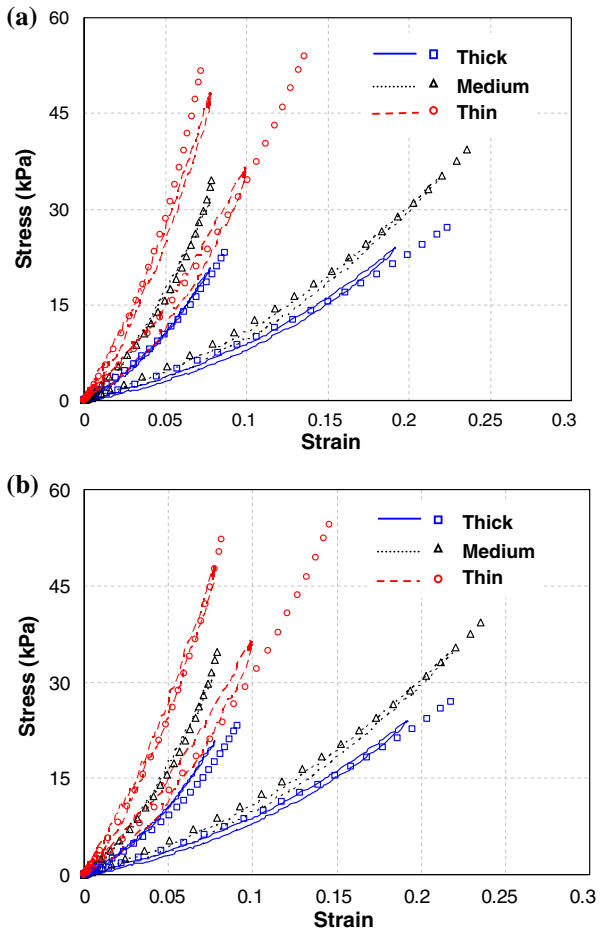

FIGURE 11. Simulation results of Cauchy stress vs. logarithmic strain for elastin network along the thoracic aorta, represented by symbols. Experimental results from Fig. 9 were shown for the purpose of comparison and represented by lines. (a) Effects of cross-linking density with material parameters listed in Table 1 and (b) effects of fiber orientation with material parameters listed in Table 2.

smaller N indicates the material has more cross-linked microstructure and is less extensible.

The effect of elastin fiber orientation on the mechanical properties of elastin network can by studied by adjusting the values of a, b and c, while keeping both n and N unchanged. The material parameters are summarized in Table 2 and the results are shown in Fig. 11b ($r^2 = 0.9732 \pm 0.0282$). The ratios between eight-chain unit cell dimensions a, b, c reflects the angles between the elastin fibers. Based on the material parameters listed in Table 2, it can be seen that for thinner sections, fibers are less oriented in the radial direction, which might because that the fiber networks are more packed in the thickness direction of the thinner section. The change in fiber orientation results in significantly different stress–strain responses. Although the reason that the mechanical properties of elastin vary along the thoracic aorta is unknown, results in Fig. 11 reflect the capability of the microstructural finite element model in incorporating quantitative biophysical and there-dimensional imaging analysis in future studies.

TABLE 2. Material parameters used to simulate the stress–strain responses of elastin networks from the thick, medium, and thin sections in Fig. 11b.

	n (1/mm^3)	a	b	c	N
Thick	5.80×10^{15}	1.26	1.689	1.4	1.6
Medium	5.80×10^{15}	1.31	1.8011	1.2	1.6
Thin	5.80×10^{15}	1.62	1.8311	0.65	1.6

Both material parameters n and N are kept unchanged, while a, b, and c are allowed to change to study the effects of fiber orientation on the mechanical properties of elastin network.

CONCLUSIONS

The mechanical responses of elastin network from bovine thoracic aorta under biaxial loading were studied both experimentally and theoretically. The experimental and modeling results were presented with the goal of relating the material parameters in the microstructural model to the macroscopic mechanical properties of elastin network. It is demonstrated, for the first time, that isolated elastin from thoracic bovine aorta possesses anisotropic mechanical behavior. Experimental results show that elastin is mainly responsible for the linear elastic response at lower stress in the aortic wall. The mechanical properties of elastin vary significantly along the thoracic aorta with an increase of tangent modulus in both the longitudinal and circumferential directions from proximal to distal end. Biological assay results show that this behavior is not due to the change of elastin contents. Possible causes such as increase of cross-linking density and less radial fiber distribution in the thinner sections were discussed and modeled. Future studies combined with quantitative biophysical and there-dimensional imaging analysis are underway. Although bovine elastin network was used in this study, the general method developed here can be combined with animal models of diseases or *in vivo* imaging to gain in-depth understanding on the ECM mechanobiology in vascular remodeling.

ACKNOWLEDGMENTS

This work was supported in part by funding from NSF (0700507) and the College of Engineering at Boston University.

REFERENCES

[1]Adamczyk, M. M., T. C. Lee, and I. Vesely. Biaxial strain properties of elastase-digested porcine aortic valves. *J. Heart Valve Dis*. 9:445–453, 2000.

[2]Arruda, E. M., and M. C. Boyce. A three-dimensional constitutive model for the large stretch behavior of rubber elastic materials. *J. Mech. Phys. Solids* 41:389–412, 1993.

[3]Bischoff, J. E., E. A. Arruda, and K. Grosh. A microstructurally based orthotropic hyperelastic constitutive law. *J. Appl. Mech*. 69:570–579, 2002.

[4]Black, L. D., P. G. Allen, S. M. Morris, P. J. Stone, and B. Suki. Mechanical and failure properties of extracellular matrix sheets as a function of structural protein composition. *Biophys. J*. 94:1916–1929, 2008.

[5]Daamen, W. F., T. Hafmans, J. H. Veerkamp, and T. H. van Kuppevelt. Comparison of five procedures for the purification of insoluble elastin. *Biomaterials* 22:1997–2005, 2001.

[6]Daamen, W. F., H. T. B. van Moerkerk, T. Hafmans, L. Buttafoco, A. A. Poot, J. H. Veerkamp, and T. H. van Kuppevelt. Preparation and evaluation of molecularly-defined collagen–elastin–glycosaminoglycan scaffolds for tissue engineering. *Biomaterials* 24:4001–4009, 2003.

[7]Daamen, W. F., J. H. Veerkamp, J. C. M. van Hest, and T. H. van Kuppevelt. Elastin as a biomaterial for tissue engineering. *Biomaterials* 28:4378–4398, 2007.

[8]Delfino, A., N. Stergiopulos, J. E. Moore, and J. J. Meister. Residual strain effects on the stress field in a thick wall finite element model of the human carotid bifurcation. *J. Biomech*. 30:777–786, 1997.

[9]Flory, P. J., and J. Rehner. Statistical mechanics of cross-linked polymer networks: I. Rubber elasticity. *J. Chem. Phys*. 11:512–520, 1943.

[10]Fung, Y. C., K. Fronek, and P. Patitucci. Pseudoelasticity of arteries and the choice of its mathematical expression. *Am. J. Physiol*. 237:H620–H631, 1979.

[11]Gilbert, T. W., M. S. Sacks, J. S. Grashow, S. L. Y. Woo, S. F. Badylak, and M. B. Chancellor. Fiber kinematics of small intestinal submucosa under biaxial and uniaxial stretch. *J. Biomech. Eng*. 128:890–898, 2006.

[12]Gundiah, N., M. B. Ratcliffe, and L. A. Pruitt. Determination of strain energy function for arterial elastin: experiments using histology and mechanical tests. *J. Biomech*. 40:586–594, 2007.

[13]Holzapfel, G. A., and T. C. Gasser. A new constitutive framework for arterial wall mechanics and a comparative study of material models. *J. Elast*. 61:1–48, 2000.

[14]Huang, W., D. Delgado-West, J. T. Wu, and Y. C. Fung. Tissue remodeling of rat pulmonary artery in hypoxic breathing. II. Course of change of mechanical properties. *Ann. Biomed. Eng*. 29:552–562, 2001.

[15]Humphrey, J. D. Mechanics of arterial wall: review and directions. *Crit. Rev. Biomed. Eng*. 23:1–162, 1995.

[16]James, H. M., and E. Guth. Theory of the elastic properties of rubber. *J. Chem. Phys*. 10:455–481, 1943.

[17]Kielty, C. M., M. J. Sherratt, and C. A. Shuttleworth. Elastic fibers. *J. Cell Sci*. 115:2817–2828, 2002.

[18]Knezevic, V., A. J. Sim, T. K. Borg, and J. W. Holmes. Isotonic biaxial loading of fibroblast-populated collagen gels: a versatile, low-cost system for the study of mechanobiology. *Biomech. Model. Mechanobiol*. 1:59–67, 2002.

[19]Kurane, A., D. T. Simionescu, and N. R. Vyavahare. In vivo cellular repopulation of tubular elastin scaffolds mediated by basic fibroblast growth factor. *Biomaterials* 28(18):2830–2838, 2007.

[20]Lally, C., A. J. Reid, and P. J. Prendergast. Elastic behavior of porcine coronary artery tissue under uniaxial and equibiaxial tension. *Ann. Biomed. Eng*. 32:1355–1364, 2004.

[21]Lillie, M. A., and J. M. Gosline. The effects of hydration on the dynamic mechanical properties of elastin. *Biopolymers* 29:1147–1160, 1990.

[22]Lillie, M. A., and J. M. Gosline. The viscoelastic basis for the tensile strength of elastin. *Int. J. Biol. Macromol*. 30:119–127, 2002.

[23]Lillie, M. A., and J. M. Gosline. Mechanical properties of elastin along the thoracic aorta in the pig. *J. Biomech*. 10:2214–2221, 2007.

[24]Lillie, M. A., and J. M. Gosline. Limits to the durability of arterial elastin tissue. *Biomaterials* 28:2021–2031, 2007.

[25]Lin, A. P., E. Bennett, L. E. Wisk, M. Gharib, S. E. Fraser, and H. Wen. Circumferential strain in the wall of the common carotid artery: comparing displacement-encoded and cine MRI in volunteers. *Magn. Reson. Med*. 60:8–13, 2008.

[26]Lu, Q., K. Ganesan, D. T. Simionescu, and N. R. Vyavahare. Novel porous aortic elastin and collagen scaffolds for tissue engineering. *Biomaterials* 25:5227–5237, 2004.

[27]McEniery, C. M., I. B. Wilkinson, and A. P. Avolio. Age, hypertension, and arterial function. *Clin. Exp. Pharmacol. Physiol*. 34:665–671, 2007.

[28]Mecham, R. P. Methods in elastic tissue biology: elastin isolation and purification. *Methods* 45:32–41, 2008.

[29]Poiani, G. J., C. A. Tozzi, S. E. Yohn, R. A. Pierce, S. A. Belsky, R. A. Berg, S. Y. Yu, S. B. Deak, and D. J. Riley. Collagen and elastin metabolism in hypertensive pulmonary arteries of rats. *Circ. Res*. 66:968–978, 1990.

[30]Rasmussen, B. L., E. Bruenger, and L. B. Sandberg. A new method for purification of mature elastin. *Anal. Biochem*. 64:225–229, 1975.

[31]Rezakhaniha, R., and N. Stergiopulos. A structural model of the venous wall considering elastin anisotropy. *J. Biomech. Eng*. 130:031017, 2008.

[32]Sacks, M. S., and C. J. Chuong. Biaxial mechanical properties of passive right ventricular free wall myocardium. *J. Biomech. Eng*. 114:183–190, 1992.

[33]Sacks, M. S., and W. Sun. Multiaxial mechanical behavior of biological materials. *Annu. Rev. Biomed. Eng*. 5:251–284, 2003.

[34]Schwartz, C. J., A. J. Valente, E. A. Sprague, J. L. Kelley, and R. M. Nerem. The pathogenesis of atherosclerosis: an overview. *Clin. Cardiol*. 14:11–16, 1991.

[35]Simionescu, D. T., Q. Lu, Y. Song, S. J. Lee, T. N. Rosenbalm, C. Kelley, and N. R. Vyavahare. Biocompatibility and remodeling potential of pure arterial elastin and collagen scaffolds. *Biomaterials* 27:702–713, 2006.

[36]Takamizawa, K., and K. Hayashi. Strain energy density function and uniform strain hypothesis for arterial mechanics. *J. Biomech*. 20:7–17, 1987.

[37]Todorovich-Hunter, L., D. J. Johnson, P. Ranger, F. W. Keeley, and M. Rabinovitch. Altered elastin and collagen synthesis associated with progressive pulmonary hypertension induced by monocrotaline: a biochemical and ultrastructural study. *Lab. Invest*. 58:184–195, 1988.

[38]Watson, R. E. B., C. E. M. Griffiths, N. M. Craven, C. A. Shuttleworth, and C. M. Kielty. Fibrilin-rich microfibrils are reduced in photoaged skin. Distribution at the dermal-epidermal junction. *J. Invest. Dermatol*. 112:782–787, 1999.

[39]Wedding, K. L., M. T. Draney, R. J. Herfkens, C. K. Zarins, C. A. Taylor, and N. J. Pelc. Measurement of vessel wall strain using cine phase contrast MRI. *J. Magn. Reson. Imaging* 15:418–428, 2002.

[40]Wells, S. M., B. L. Langille, and J. M. Lee. In vivo and in vitro mechanical properties of the sheep thoracic aorta in the perinatal period and adulthood. *Am. J. Physiol.* 274:1749–1960, 1998.

[41]Wells, S. M., B. L. Langille, J. M. Lee, and S. L. Adamson. Determinants of mechanical properties in the developing ovine thoracic aorta. *Am. J. Physiol.* 277:1385–1391, 1999.

[42]Wolinsky, H. Effects of hypertension and its reversal on the thoracic aorta of male and female rats. Morphological and chemical studies. *Circ. Res.* 28:622–637, 1971.

[43]Wuyts, F. L., V. J. Vanhuyse, G. J. Langewouters, W. F. Decraemer, E. R. Raman, and S. Buyle. Elastic properties of human aortas in relations to age and atherosclerosis: a structural model. *Phys. Med. Biol.* 40:1577–1597, 1995.

[44]Zhang, Y., M. L. Dunn, E. S. Drexler, C. N. McCowan, A. J. Slifka, D. D. Ivy, and R. Shandas. A microstructural hyperelastic model of pulmonary arteries under normo- and hypertensive conditions. *Ann. Biomed. Eng.* 33:1042–1052, 2005.

[45]Zhou, J., and Y. C. Fung. The degree of nonlinearity and anisotropy of blood vessel elasticity. *Proc. Natl. Acad. Sci. U.S.A.* 94:14255–14260, 1997.